The International Journal of Advanced Manufacturing Technology (2019) 100:729–740
https://doi.org/10.1007/s00170-018-2706-2

ORIGINAL ARTICLE

Effects of mechanical property parameters on wrinkling behavior of thin-walled tubes in hydroforming process

Xiao-Lei Cui [1,2] · Xiao-Song Wang [2] · S. J. Yuan [2]

Received: 25 May 2018 / Accepted: 17 September 2018 / Published online: 27 September 2018

Abstract

In tube hydroforming, some controllable wrinkles can be used to improve the formability of tubes, so as to obtain the tubular parts with large expansion ratio and relatively uniform wall thickness. In this paper, finite element analysis and experimental research with 5052 aluminum alloy and 304 stainless steel tubes are used to investigate the effects of mechanical property parameters on wrinkling behavior of thin-walled tubes for hydroforming application. The numerical simulation results show that the effect of elastic modulus is very small and ignorable, but the initial yield stress and tangent modulus of tubes have an obvious effect on their wrinkling behavior. Tubes with higher initial yield stress and lower tangent modulus tend to possess three axisymmetric wrinkles within the lower internal pressure range. Moreover, it is found that the ratio of initial yield stress to flow stress of the tubes, σ_s/σ_f, is a significant factor to their wrinkling behavior. Three axisymmetric wrinkles could be produced on the tubes with higher σ_s/σ_f under a lower internal pressure. All of these were verified by the experimental results of 5052 aluminum alloy and 304 stainless steel tubes, whose wrinkles obtained under wrinkling internal pressure of 1.8 p_s and 1.2 p_s can be flattened completely in the calibration stage. These research findings are extremely meaningful to get controllable wrinkles for different kinds of tubes.

Keywords Wrinkling · Tube hydroforming · Mechanical property parameters · Thin-walled tubes · Axial feeding · Internal pressure

1 Introduction

In recent years, the light alloys, such as aluminum alloys [1, 2] and magnesium alloys [3, 4], have received enough attention for their lightweight and high specific strength, which are beneficial to the reduction of fuel consumption. In order to manufacture an aluminum alloy or magnesium alloy hollow-structure component for the automobile or aircraft, tube hydroforming technology can be a good choice [5]. However, the low ductility and work hardening capacity of the light alloy tubes remain obstacles for their successful hydroforming. For these tubes, several kinds of failure, such as localized wrinkling and bursting, may occur on the tubes during the hydroforming process [6]. Almost all the efforts in the past were made to avoid the defects of wrinkling or bursting as far as possible in tube hydroforming, and the hydroforming was suggested to be conducted in the optimized process window diagram [7].

While most researchers in the hydroforming field focus on avoiding wrinkling defect, Yuan et al. [8] do the opposite. They found that some wrinkles can be controlled and used in hydroforming to improve the formability of tubes. These wrinkles should be preformed to accumulate tube materials in the expansion zone under an optimal loading path, and then, they are flattened completely in the subsequent calibration stage. Until now, some preliminary works about the wrinkle formation and their flattening behavior have been conducted, to explore the wrinkling instability behavior for hydroforming application. Lang et al. [9] used the useful wrinkles to hydroform an aluminum alloy variable-diameter tube firstly. They investigated numerically the effect of internal pressure on wrinkling behavior and found that four preformed wrinkles can be flattened completely in calibration stage, but it showed a wrinkle on the hydroformed part in the experiment. Lang et al. [10] also used the useful wrinkles in multi-stage hydroforming of aluminum alloy tube. Both of the wrinkling

✉ Xiao-Lei Cui
cuixiaolei2005@163.com; cuixiaolei@tyut.edu.cn

[1] College of Materials Science and Engineering, Taiyuan University of Technology, Taiyuan 030024, People's Republic of China

[2] National Key Laboratory for Precision Hot Processing of Metals, Harbin Institute of Technology, Harbin 150001, People's Republic of China

and flattening behavior in preforming stage and calibration stage, as well as the suitable preforming die cavity shape, were discussed numerically. In order to improve the hydroformability, Song et al. [11] introduced a novel numerical approach as an effective tool to design the preformed shape based on the deformation history. Here, the preformed shape is actually the useful wrinkles that can be flattened completely in the finial target shape. Besides, wrinkling and flattening behavior of magnesium alloy tubes at elevated temperatures was also investigated experimentally by Tang et al. [12]. All of these investigations told a truth that the expansion ratio of the tubular parts formed using useful wrinkles could be larger, and the wall thickness distribution in the expanding area will be more uniform [13].

Even though a series of numerical simulations and experiments for wrinkling behavior of tubes have been conducted, it still lacks the systematic knowledge about the dependence of wrinkling behavior on the process parameters, material parameters, and the geometric parameters of tubes. It could not suggest the general procedure for wrinkles preforming as well. Recently, the wrinkling behavior of thin-walled tubes under complex stress states, especially under double-sided pressures, was investigated by Yuan et al. [14] and Cui et al. [15]. The effect of external pressure has been discussed under three cases, and the shape of wrinkles was fitted effectively using the GaussAmp function. On this basis, Wang et al. [16] studied the flattening behavior of wrinkles in the calibration stage and obtained the geometry unfolding conditions for the useful wrinkles. However, these finished works are not a sufficient solution for the preforming of useful wrinkles with all kinds of tube materials. It is necessary to point out the influence factors on the wrinkling behavior in detail, so that the reasonable preformed wrinkles and the required loading path can be designed efficiently once a new tube material will be used.

In this paper, it is devoted to investigate the effects of mechanical property parameters on wrinkling behavior of thin-walled tubes for hydroforming application. Firstly, the finite element analysis was used to give a clear explanation on the effects of elastic modulus, initial yield stress, and tangent modulus on the wrinkling behavior. Then, 5052 aluminum alloy tubes and 304 stainless steel tubes were used in the wrinkling experiments. Difference of wrinkling behavior between these two tubes, as well as the flattening behavior of wrinkles, is compared and discussed in detail.

2 Preparations

2.1 Materials

The as-received tube materials used in this investigation are 5052 aluminum alloy tube and 304 stainless steel tube. This is because these two kinds of tubes are commonly used in the industry, and they have large difference regarding the elastic modulus, yield stress, and hardening characteristic. It can be better to show the effect of mechanical property parameters on the wrinkling behavior. The two kinds of tubes have the identical outer diameter of 63 mm and nominal thickness of 2 mm. The 5052 aluminum alloy tube was drawn from extruded tube and then annealed at 380 °C for about 2 h, while the 304 stainless steel tube was hot-rolled samples. The uniaxial tensile tests were conducted on an Instron 5569 machine along the axial direction of the two kinds of tube materials respectively. Their true stress-strain curves are shown in Fig. 1 and the corresponding mechanical parameters are listed in Table 1. Both of the true stress-strain curves are fitted using the Hollomon equation, and the strength coefficient K and strain hardening exponent n for two tubes are given in Fig. 1.

2.2 Experimental setup

The experimental setup shown in Fig. 2 was designed and manufactured for the investigation of wrinkling behavior of thin-walled tubes in hydroforming process. The hydroforming die is mainly composed of upper die, lower die, left punch, and right punch. After the die is closed, the wrinkles are developed under the combined action of internal pressure and axial feeding. The hydraulic booster is used to supply the internal pressure, and the hydraulic cylinder is used to perform the axial feeding. They are both controlled by servo valves. It can be seen that the maximum diameter of the die cavity is 85 mm, and its length is 63 mm. The half conical angle of the transition zone was designed as 20°, and a total length of 123.5 mm for the deformation area was obtained. The experimental investigations into wrinkling behavior of tubes were carried out on the 20-MN hydroforming press at Harbin Institute of Technology, and more information about this

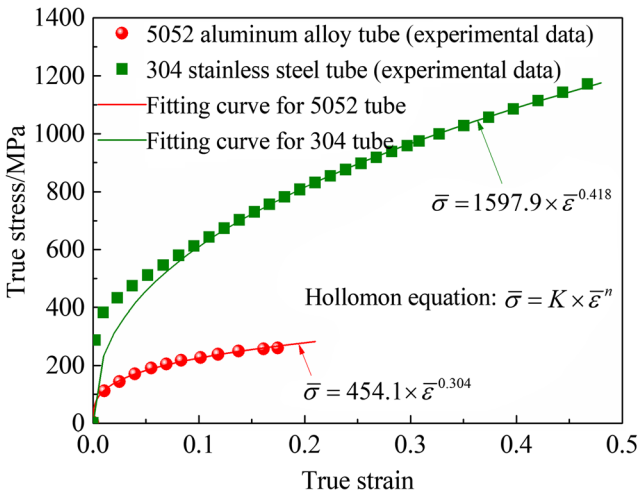

Fig. 1 True stress-strain curve of as-received tube materials along the axial direction

Table 1 Mechanical parameters of as-received tube materials along the axial direction

Mechanical parameters	Value	
	5052 tube	304 tube
Elastic modulus, E (GPa)	70 [17]	210 [18]
Initial yield stress, σ_s (MPa)	85.9	351.5
Ultimate tensile strength, σ_b (MPa)	222.9	731.3
Total elongation, δ_u (%)	26.1	68.6
Uniform elongation, δ (%)	18.2	61.1

experimental setup has been discussed by Yuan et al. [14] in the previously published papers.

2.3 Finite element model

In view of geometrical characteristics of the circular tube and the shape of die cavity in Fig. 2, an axisymmetric model was developed in Abaqus/Explicit to investigate the shape and dimensions of wrinkles on the tube, as shown in Fig. 3. The tubes are assigned to obey the Mises yield criterion $\overline{\sigma} = \{[(\sigma_1-\sigma_2)^2 + (\sigma_2-\sigma_3)^2 + (\sigma_3-\sigma_1)^2]/2\}^{1/2} = \{[(\sigma_x-\sigma_y)^2 + (\sigma_y-\sigma_z)^2 + (\sigma_z-\sigma_x)^2 + 6(\tau_{xy}^2 + \tau_{yz}^2 + \tau_{zx}^2)]/2\}^{1/2}$ and the elastic-plastic material model in these simulations. The CAX4R elements (a 4-node bilinear axisymmetric quadrilateral, reduced integration, hourglass) were assigned to the deformable tube, and the die was defined as an analytical rigid shell. For the initial tube with a total length of 210 mm, the element size was set as 0.2 mm, so there are ten elements in thickness direction of the tube and its total number of grid is 10,500.

A constant pressure was imposed on the internal surface of the tube along with the axial feeding of left and right punches. In regard to the tube/die and tube/punches interaction, a surface-to-surface contact with friction coefficients of 0.125 was applied [19]. In addition, a self-contact interaction was appointed on the inside surface and outside surface of the tube to simulate the possible wrinkles folding.

2.4 Research procedure

This investigation is achieved using the numerical simulation and experimental verification and divided into two stages: firstly, the numerical simulation was conducted to reveal the effects of mechanical property parameters, including elastic modulus, initial yield stress, and tangent modulus, on the wrinkling behavior of thin-walled tubes. For simplicity, the ideal linear strengthening elastic-plastic model, i.e., the bilinear hardening model, was used in the numerical simulation, as shown in Fig. 4. Note that if the tangent modulus during the plastic deformation stage, E_t, is assumed to be 0, it returns to the ideal elastoplastic model. In this simulation, different levels of elastic modulus, initial yield stress, and tangent modulus are assigned to the tube respectively, as shown in Table 2. In Table 2, the values of elastic modulus were selected based on the frequently used magnesium alloy, aluminum alloy, and steel. The values of initial yield stress and tangent modulus were determined optionally, not aiming at a certain material.

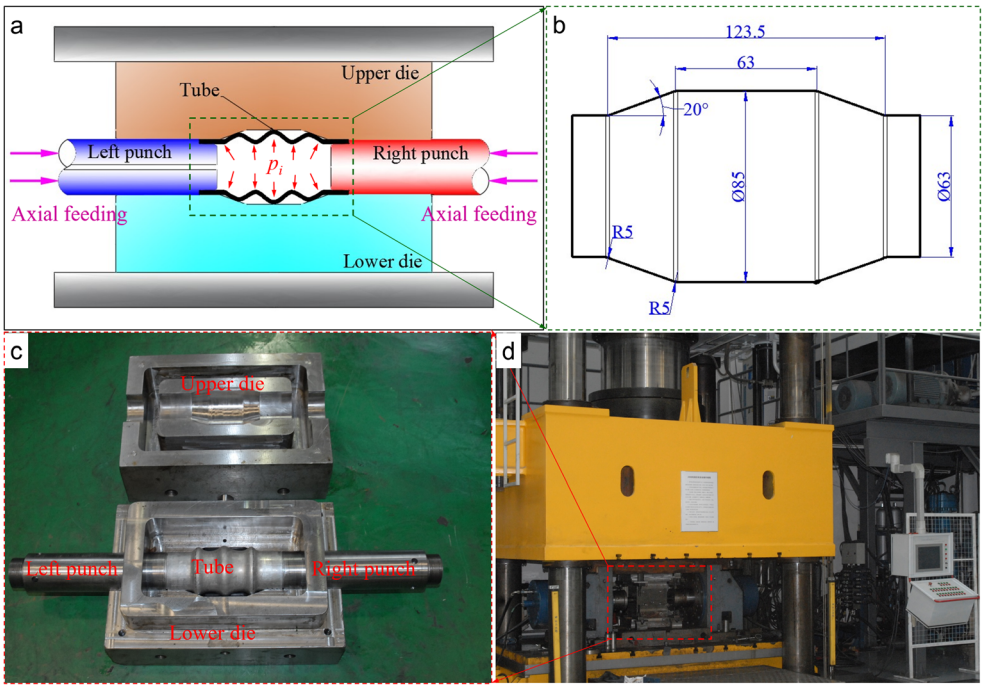

Fig. 2 Experimental setup: **a** schematic diagram of wrinkling in tube hydroforming; **b** dimension of the die cavity; **c** experimental die for the wrinkling of tubes; **d** 20-MN hydroforming press

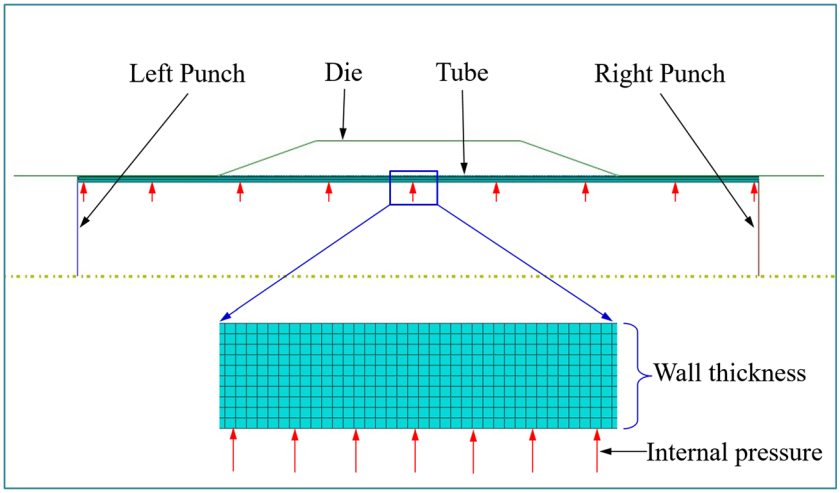

Fig. 3 Finite element model for the wrinkling during hydroforming process

Secondly, the 5052 aluminum alloy tubes and the 304 stainless steel tubes are used to make the experimental comparative study of wrinkling behavior.

Figure 5 shows the schematic of loading paths for the wrinkling formation during tube hydroforming. The liquid should be pressurized to the desired level firstly for the buildup of internal pressure (T_0–T_1). Then, in the subsequent wrinkling stage (T_1–T_2), the internal pressure remains unchanged while the left and right punches are advanced to push the tube into the die cavity for the wrinkle formation. Both in experiments and simulations, a total stroke of 30 mm, i.e., a feeding ratio of 80% compared with the ideal feeding amount, was implemented by the left and right punches. This feeding amount was determined based on the geometrical analysis of wrinkling in published papers [8, 16]. For the constant internal pressure during wrinkling stage, it was set to different values among 0.4 p_s, 0.6 p_s, 0.8 p_s, 1.0 p_s, 1.2 p_s, 1.4 p_s, 1.6 p_s, and 1.8 p_s, where p_s represents the initial yield pressure of the tube which can be calculated by the Tresca yield function ($\sigma_1 - \sigma_3 = \sigma_s = 2k$ ($\sigma_1 > \sigma_2 > \sigma_3$)). For more information about the loading paths, it can be referred to the previously published papers [16].

Furthermore, in order to verify the feasibility of useful wrinkles for hydroforming application with different tubes, the wrinkled 5052 and 304 tubes are bulged toward to the die cavity under higher internal pressure. In the calibration process, a defect-free tubular specimen will be obtained if the wrinkles could be flattened completely to match the die cavity.

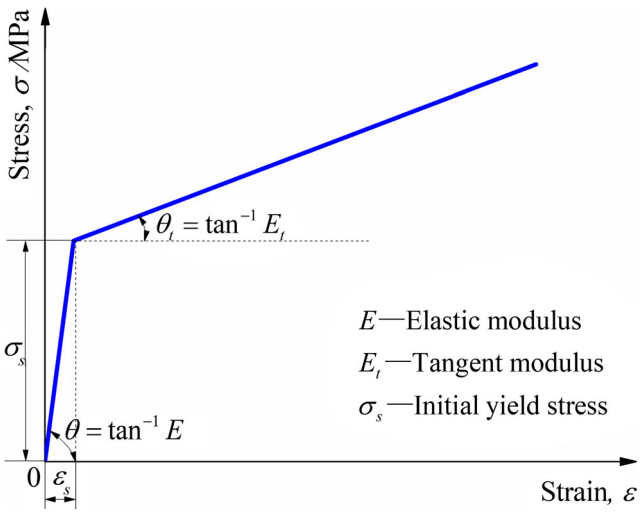

Fig. 4 Ideal linear strengthening elastic-plastic model

3 Results and discussion

3.1 Effect of elastic modulus on wrinkling behavior

Figure 6 shows the effect of elastic modulus on the contours and shape of wrinkled tubes under different internal pressures after wrinkling process. The color contours represent the radial displacement of the wrinkles U1, in which the dark gray with a negative displacement value shows the occurrence of

Table 2 Mechanical property parameters used in the finite element simulation for the investigation of their influence

Mechanical parameters	Elastic modulus E (GPa)	Initial yield stress σ_s (MPa)	Tangent modulus E_t (MPa)
Effect of elastic modulus	45	85	1000
	70	85	1000
	210	85	1000
Effect of initial yield stress	70	85	1000
	70	170	1000
	70	255	1000
Effect of tangent modulus	70	85	577
	70	85	1000
	70	85	1732

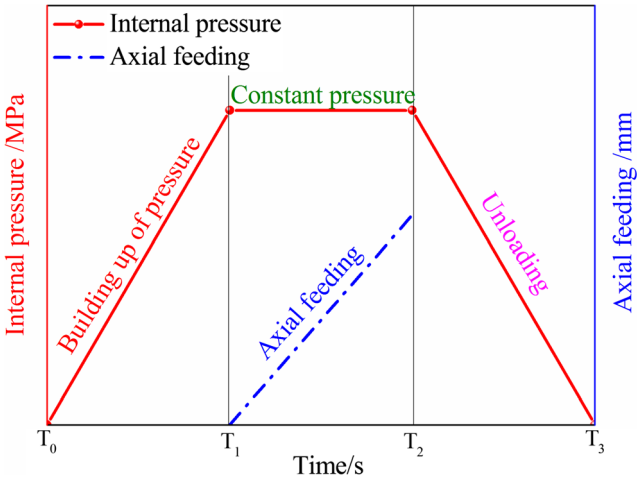

Fig. 5 Schematic of loading paths for the wrinkling formation during tube hydroforming

inward folding. It can be found from Fig. 6 that the number and shape of wrinkles have almost no dependence on the elastic modulus under different internal pressures from 0.4 to 1.8 p_s. Under relative low internal pressure (0.4 p_s), they only have two wrinkles at both ends of the deformation zone of the tube, and severe inward folding occurs near the end wrinkles. With the increasing internal pressure, three axisymmetric wrinkles are formed with a greater diameter and width.

Moreover, the wrinkle formation process under the internal pressure of 1.2 p_s is given in Fig. 7 to compare its dependence on the elastic modulus. It can be found from this figure that the effect of elastic modulus on the wrinkling behavior is negligible. In the early stage of axial feeding from 0 to 6 mm, two end wrinkles are produced and the shape of wrinkles under different elastic modulus are almost the same. When the axial feeding reaches 12 mm, the middle wrinkles appear and there is a little difference at the top of the middle wrinkles. And with the increasing axial feeding from 12 to 30 mm, the slight difference of the wrinkles moves to the bottom of the wrinkles. In a word, the shape difference is very small compared with the wrinkles themselves. It is chiefly because the strain of the tube exceeds the elastic limit during the wrinkling process, and the wrinkle formation process is actually a plastic deformation

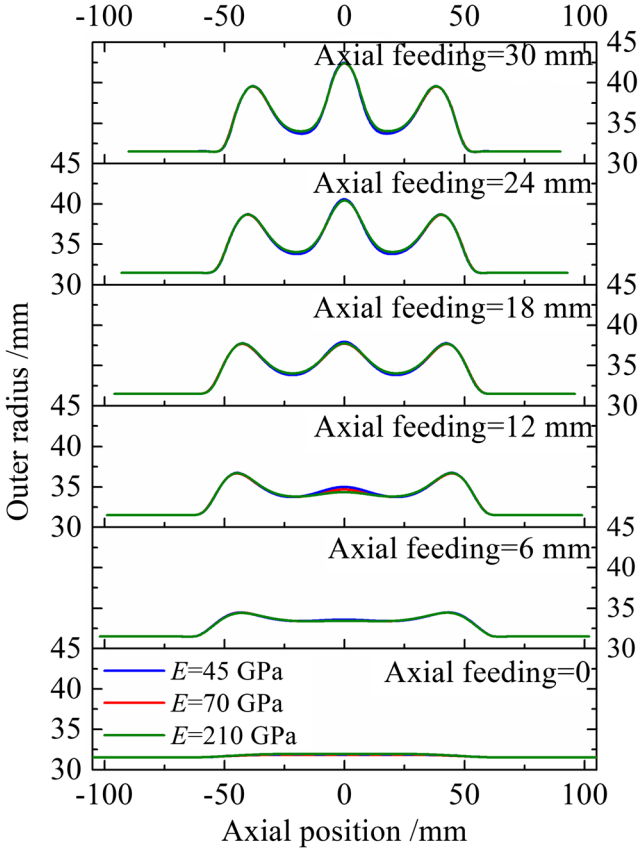

Fig. 7 Effect of elastic modulus on wrinkle formation process under internal pressure of 1.2 p_s

Fig. 6 Effect of elastic modulus on wrinkling behavior (contours of wrinkled tubes) under different internal pressures

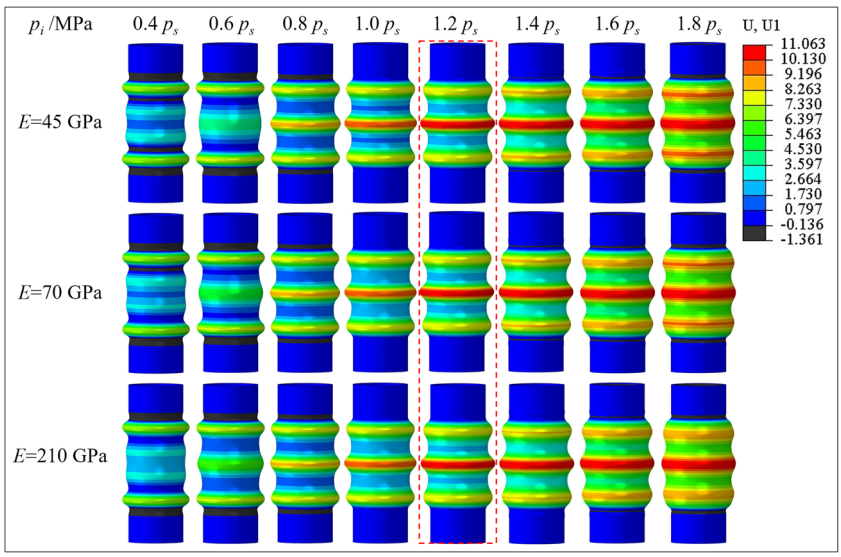

and instability process. From above, it can be concluded that effect of elastic modulus on wrinkling behavior of tubes is very small and ignorable.

3.2 Effect of initial yield stress on wrinkling behavior

Figure 8 shows the contour shape of the wrinkled tubes obtained under different initial yield stresses of 85 MPa, 170 MPa, and 255 MPa, from which the effect of initial yield stress on the wrinkling behavior under different internal pressures can be revealed. For the tubes with a yield stress of 85 MPa, three axisymmetric wrinkles can be formed under different levels of internal pressure from 0.6 to 1.8 p_s. However, if the tubes with higher yield stress were used, the internal pressure range for the formation of three axisymmetric wrinkles will be narrowed. For example, three axisymmetric wrinkles can be only formed below the internal pressure of 1.6 p_s for the tubes with a yield stress of 170 MPa. With the higher yield stress of 255 MPa, three axisymmetric wrinkles can be formed only when the internal pressure is lower than 1.2 p_s. Moreover, when the internal pressure is low enough (0.4 p_s) only two wrinkles may be formed at both ends of the deformation zone, no matter how high the initial yield stress of the tube is.

The wrinkle formation process of tubes with different initial yield stresses under internal pressure of 1.2 p_s is given in Fig. 9. Clearly, the shapes of wrinkles for these three tubes with different initial yield stresses are significantly different. For the tubes with initial yield stress of 85 MPa and 170 MPa, they both have three wrinkles, but they have different shapes. The radii of the wrinkles' top and bottom are bigger, but the distance between adjacent wrinkles is smaller when the yield stress is 170 MPa. Moreover, when the tube possesses a higher initial yield stress of 255 MPa, only two end wrinkles are formed during the wrinkling process, and then almost disappear in the remaining process. In other words, there are only slight wrinkles that can be seen for the tubes with an initial yield stress of 255 MPa when the axial feeding reaches 30 mm. In addition, more serious inward folding can be found at both ends of the wrinkling area.

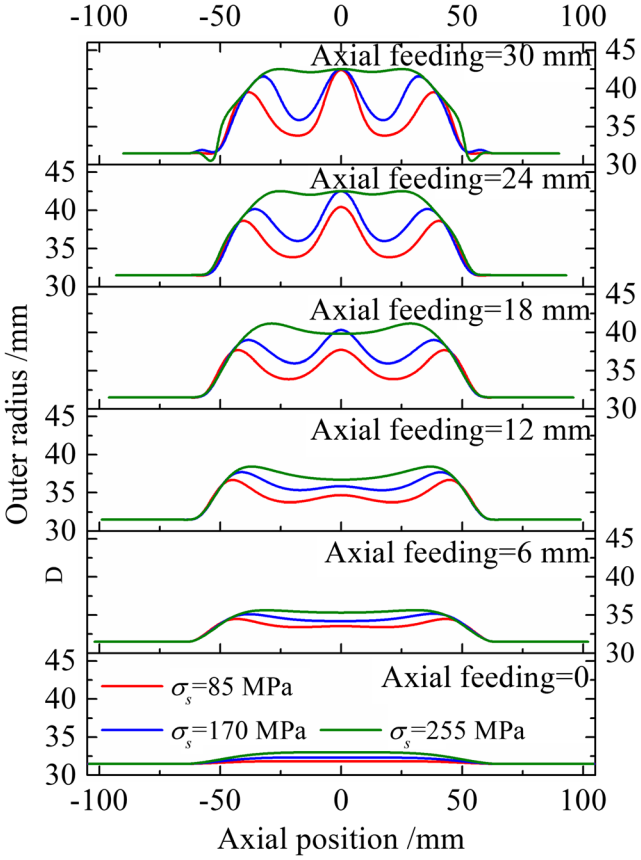

Fig. 9 Effect of initial yield stress on wrinkle formation process under internal pressure of 1.2 p_s

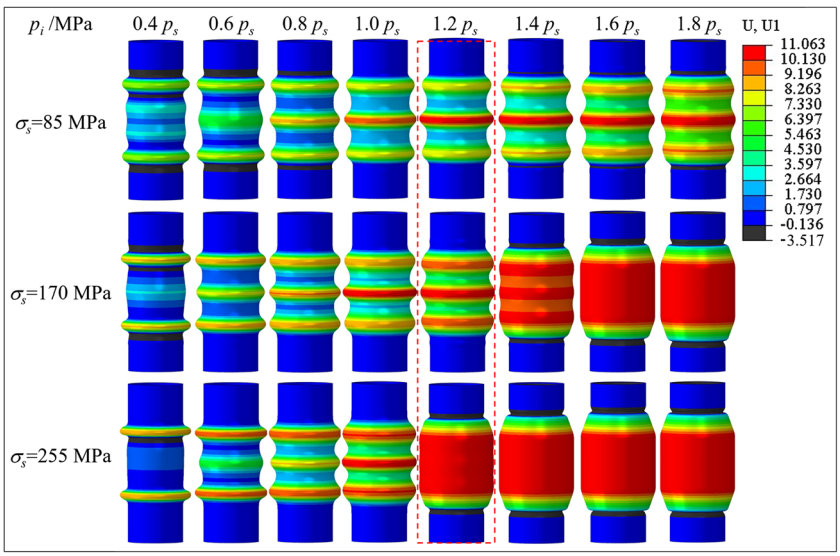

Fig. 8 Effect of initial yield stress on wrinkling behavior (contours of wrinkled tubes) under different internal pressures

During the plastic wrinkling process, the flow stress of the tube, σ_f, can be expressed as $\sigma_f = \sigma_s + \Delta\sigma$, where $\Delta\sigma$ is the increment of the equivalent stress due to working hardening of tubes. It has been concluded from the last section that the effect of elastic modulus on wrinkling behavior of tubes is very small and ignorable. On this basis, for the three tubes with different initial yield stresses, if they are assigned to have the same tangent modulus, it indicates that they will work hardening with the same $\Delta\sigma$ under the same deformation amount. Here, the ratio of initial yield stress to flow stress can be expressed as follows.

$$\sigma_s/\sigma_f = \frac{\sigma_s}{\sigma_s+\Delta\sigma} = \frac{1}{1+\frac{\Delta\sigma}{\sigma_s}} \quad (1)$$

It can be found from Eq. (1) that the tube with a higher initial yield stress has a bigger ratio of initial yield stress to flow stress, σ_s/σ_f, under the assumption of the same tangent modulus and the same deformation amount. So far, it may also be said that if the tubes with higher σ_s/σ_f were used, the internal pressure for the three axisymmetric wrinkles will be reduced.

3.3 Effect of tangent modulus on wrinkling behavior

In this section, based on the above result that the effect of elastic modulus on wrinkling behavior of tubes is very small and ignorable, the initial yield stress is fixed, and the wrinkling behavior of tubes under different tangent moduli of 577 MPa, 1000 MPa, and 1732 MPa will be discussed, as shown in Fig. 10. From Fig. 10, it can be found that the internal pressure range for the formation of three axisymmetric wrinkles will be moved to higher internal pressure with the increasing tangent modulus.

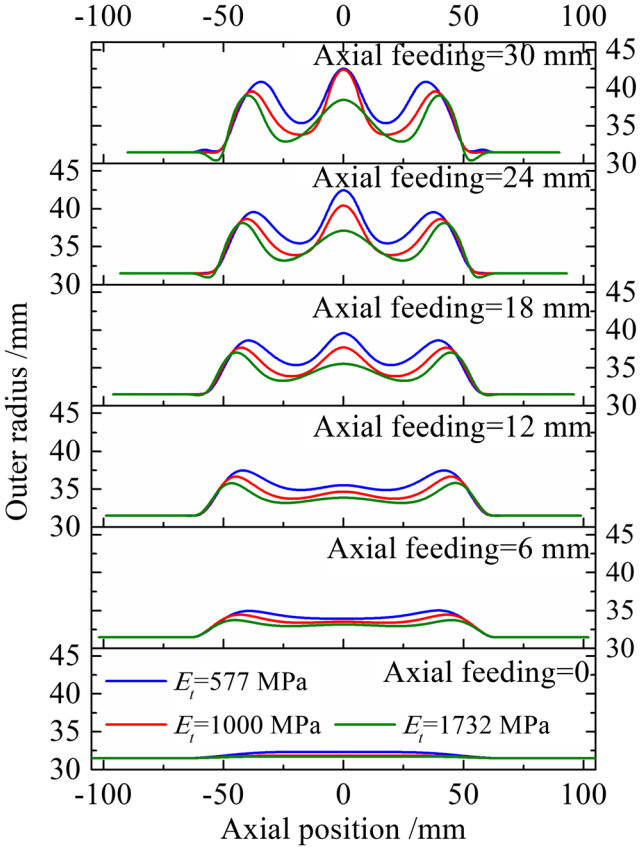

Fig. 11 Effect of tangent modulus on wrinkle formation process under internal pressure of 1.2 p_s

When the tangent modulus is 577 MPa, three axisymmetric wrinkles can be obtained only below the internal pressure of 1.4 p_s. For the higher tangent modulus of 1000 MPa and 1732 MPa, three axisymmetric wrinkles can be produced even though the internal pressure reaches 1.8 p_s, but the lower limit of internal pressure increases to 0.6 p_s and 1.2 p_s, respectively.

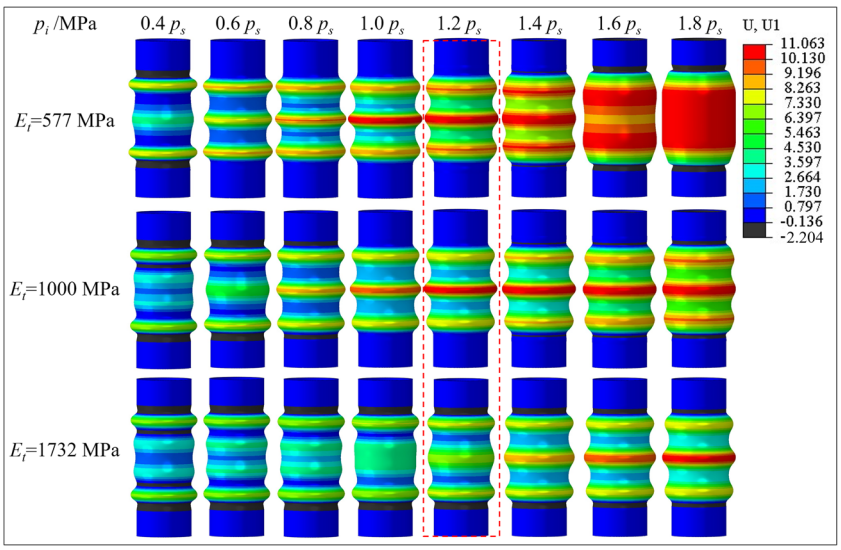

Fig. 10 Effect of tangent modulus on wrinkling behavior (contours of wrinkled tubes) under different internal pressures

Figure 11 shows the wrinkle formation process of tubes with different tangent moduli of 577 MPa, 1000 MPa, and 1732 MPa under internal pressure of 1.2 p_s. It can be seen from Fig. 11 that the radii of the wrinkle's both top and bottom decrease with the increasing tangent modulus, but the distance between adjacent wrinkles increase. All of these results indicate that the tangent modulus and initial yield stress have an opposite effect on the evolution of tube's wrinkles. This may be also related with the ratio of initial yield stress to flow stress σ_s/σ_f. With the increasing tangent modulus, the increment of the equivalent stress due to working hardening of tubes, $\Delta\sigma$, will increase under the same deformation degree. So, it can be found from Eq. (1) that the ratio of initial yield stress to flow stress, σ_s/σ_f, will reduce with the increasing tangent modulus, which is exactly the opposite of the effect of increasing initial yield stress. Therefore, it is thought that the ratio of initial yield stress to flow stress of the tubes, σ_s/σ_f, is a significant factor determining their wrinkling behavior.

In order to make a further confirmation about the dependence of wrinkling behavior of the tubes on the ratio of initial yield stress to flow stress, σ_s/σ_f, it can be verified from the opposite side. In this case, three tubes with the same σ_s/σ_f but different initial yield stress and tangent modulus were used to simulate the wrinkling behavior under the internal pressures of 0.8 p_s, 1.2 p_s, and 1.6 p_s respectively, as shown in Fig. 12. It is clearly seen from Fig. 12 that the shape and size of the wrinkles are almost the same for the tubes with the same σ_s/σ_f value. This means that once the process parameters, the dimensions of tube, and the size of die cavity have been determined, the wrinkling behavior of the tube mainly depends on the ratio of its initial yield stress to flow stress, σ_s/σ_f.

3.4 Experimental investigation of the wrinkling behavior with 5052 and 304 tubes

Figure 13 shows the wrinkled tubes of 5052 aluminum alloy and 304 stainless steel, which were obtained under different

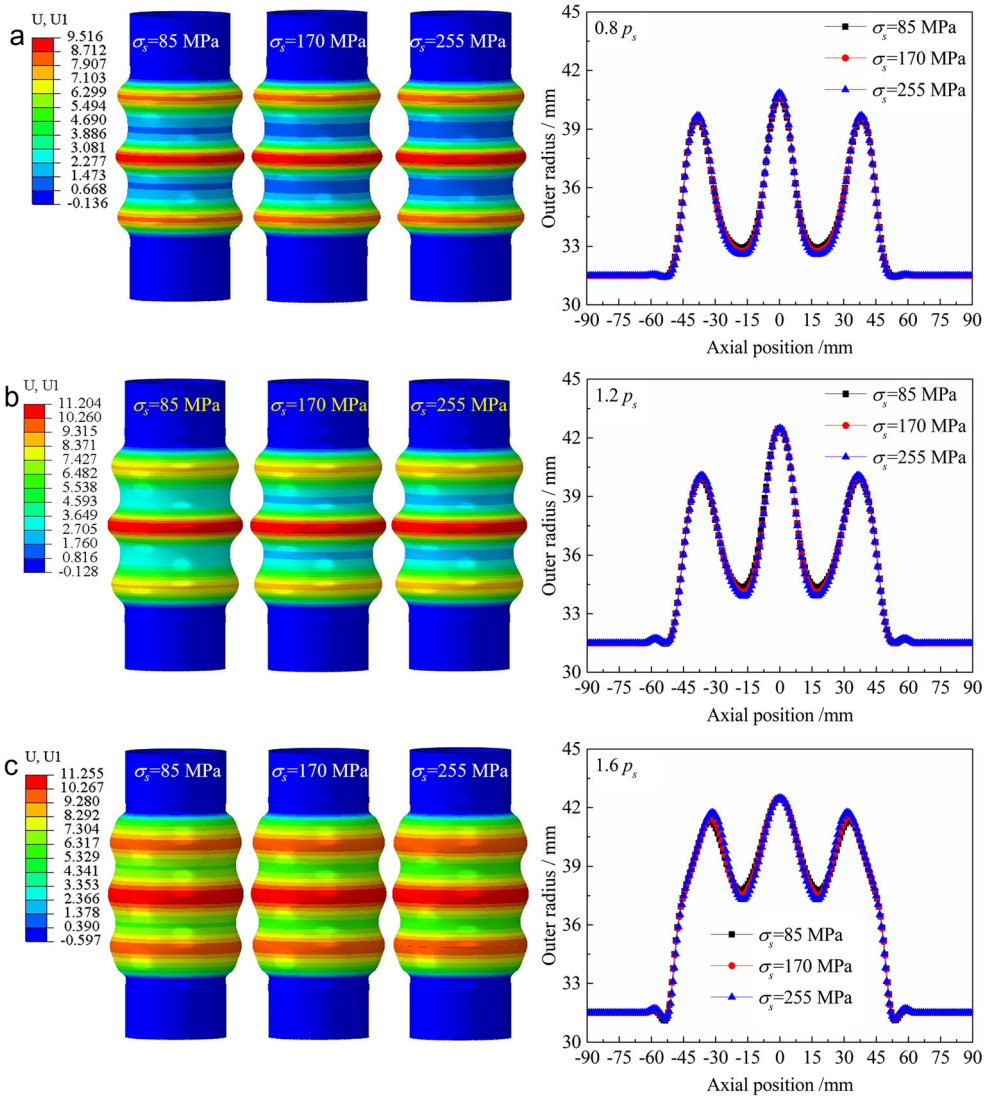

Fig. 12 Comparison of wrinkles' shape of the tubes with the same σ_s/σ_f and different initial yield stress and tangent modulus under different internal pressures: **a** 0.8p_s; **b** 1.2p_s; **c** 1.6p_s

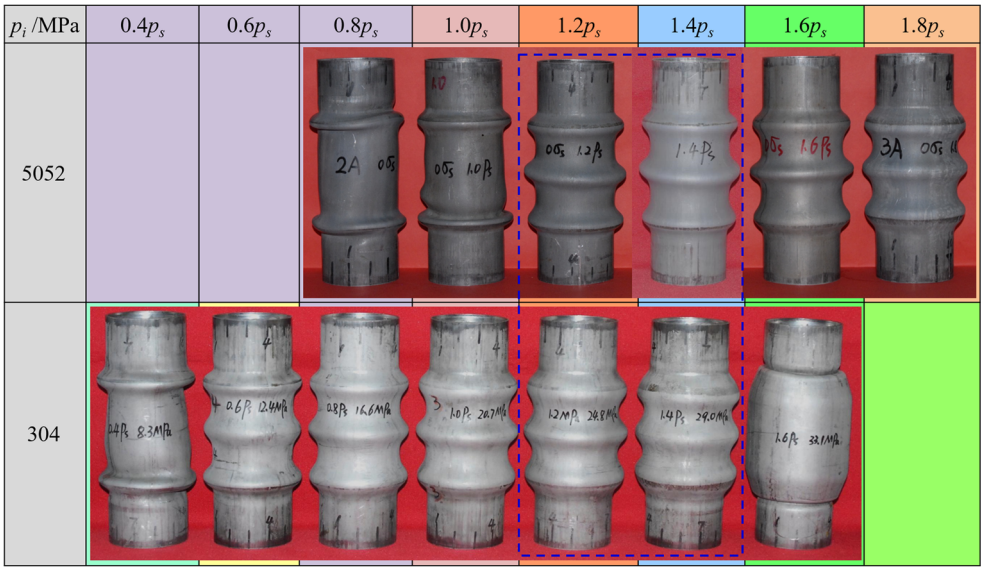

Fig. 13 Comparison of wrinkled tubes between 5052 aluminum alloy and 304 stainless steel tubes

internal pressures with the same axial feeding of 30 mm. From Fig. 13, the following results can be obtained. Firstly, the evolution of wrinkles with the increasing internal pressure for these two different tubes is approximately the same. When the internal pressure is relative low, two distorted and non-axisymmetric wrinkles are produced at the transition region of the tube. As the internal pressure continues to increase, three axisymmetric wrinkles are formed on the tube, and the three wrinkles become wider with the increasing internal pressure. For the 5052 aluminum alloy tube with low plasticity, it will fracture during the wrinkling process when the internal pressure is higher than 1.8 p_s. However, the 304 stainless steel tube is free of fracture due to its good plasticity when the internal pressure reaches 1.6 p_s, at which the 304 tube is just hydroformed to fill the die cavity without wrinkles under the combined action of internal pressure and axial feeding. The folding phenomenon at both ends is caused by the continuous advance of punches after the tube is completely filled the die cavity. Secondly, the internal pressure range for the three wrinkle formation of 304 stainless steel tube is different with that of the 5052 aluminum alloy tube. Three wrinkles can be produced in the internal pressure range of 1.2 to 1.8 p_s for the 5052 aluminum alloy tubes, but this internal pressure range for the 304 stainless steel tubes is moved to the range of 0.6 to 1.4 p_s for the formation of three wrinkles. It can be found that all of these experimental phenomena are consistent with the above numerical simulation results. From the above finite element analysis, it is concluded that tubes with higher initial yield stress and lower tangent modulus tend to possess three wrinkles within the lower internal pressure range. However, it can be found from Fig. 1 that the tangent modulus and initial yield stress of 304 stainless steel tube are both bigger than that of the 5052 aluminum alloy tube. Therefore, it cannot be pointed out whether the difference of initial yield stress or the difference of tangent modulus between 5052 aluminum alloy tube and 304 stainless steel tube causes the difference in their wrinkling behavior.

It has been presented that the ratio of tube's initial yield stress to flow stress, σ_s/σ_f, is a significant factor to its wrinkling behavior, and the internal pressure for the three wrinkles will be reduced for the tubes with higher σ_s/σ_f. Figure 14 shows the ratio of initial yield stress to flow stress for 5052 aluminum alloy and 304 stainless steel tubes. Clearly, the 304 stainless steel tube has a higher value of σ_s/σ_f than the 5052 aluminum alloy tube.

Moreover, it can be also found from Fig. 13 that width of the three wrinkles of 304 stainless steel tube is bigger than that of the 5052 aluminum alloy tube when they are formed under the internal pressure of 1.2 p_s and 1.4 p_s, respectively. It has been found that the shape of wrinkles of 5052 aluminum alloy

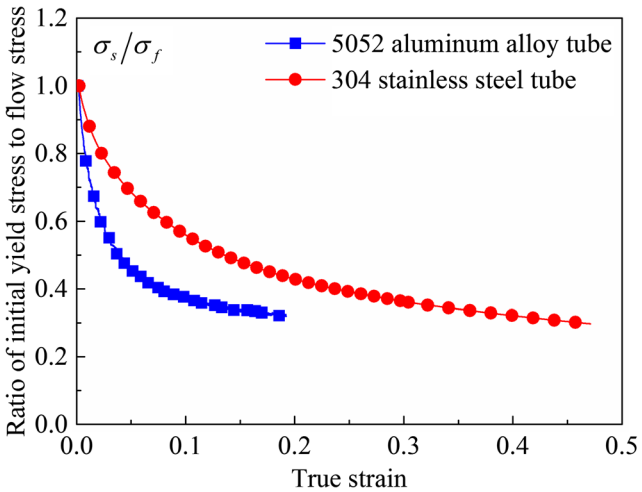

Fig. 14 Ratio of initial yield stress to flow stress for 5052 aluminum alloy and 304 stainless steel tubes

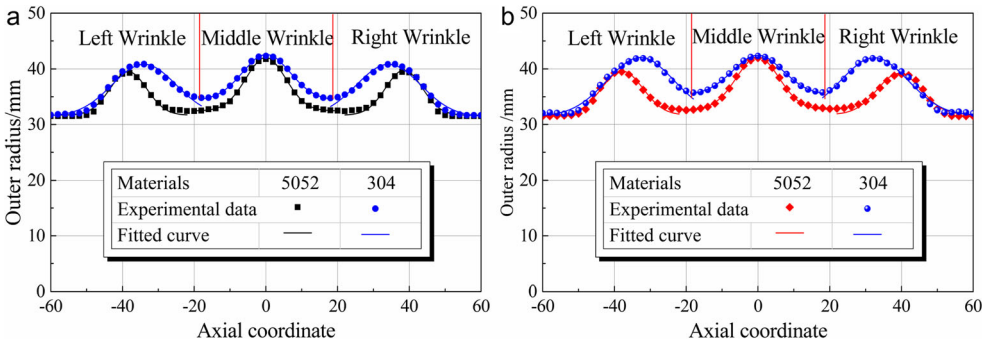

Fig. 15 Comparison of wrinkles' shape of 5052 aluminum alloy and 304 stainless steel tubes: **a** $p_i = 1.2\ p_s$; **b** $p_i = 1.4\ p_s$

tube, especially the middle wrinkle, could be described accurately using the GaussAmp function [14]. Here, the wrinkles of these two tubes under internal pressure of 1.2 p_s and 1.4 p_s were fitted using the GaussAmp function, as shown in Fig. 15. In the same time, the corresponding fitting functions have been given in Table 3. It can be found from Fig. 15 and Table 3 that both the wrinkles of 304 stainless steel tube and 5052 aluminum alloy tube can be described accurately using the GaussAmp function. Under the same yield pressure, the wrinkle's width and bottom radius of 304 stainless steel tube are bigger than those of 5052 aluminum alloy tube. When the internal pressures are 1.2 p_s and 1.4 p_s, the bottom radius of wrinkles for 5052 aluminum alloy tube is 32.454 mm and 32.672 mm, respectively, while for 304 stainless steel tube is 34.389 mm and 35.359 mm, respectively. Besides, the distance between left and right wrinkles for 304 stainless steel tube is shorter than that of the 5052 aluminum alloy tube. All of these wrinkling laws in the experiment agree with Figs. 9 and 11.

3.5 Flattening of the tube's wrinkles

To apply wrinkling behavior of tubes in hydroforming, the wrinkles should be flattened under higher internal pressure in the calibration process. Therefore, the wrinkled tubes of 5052 aluminum alloy tubes and 304 stainless steel tubes in Fig. 13 were hydroformed under a higher internal pressure of 80 MPa and 200 MPa, respectively, so as to reveal the effect of mechanical properties on their flattening behavior. The flattened results of these two tubes are shown in Fig. 16.

It can be found from Fig. 16 that the flattening behavior of 304 stainless steel tube is basically the same as that of the 5052 aluminum alloy tube. With a relative low internal pressure for wrinkling, the wrinkled tube will fracture during the flattening process due to the lack of sufficient materials in the middle of the tube. The flattening results will become better without any fracture with the increasing internal pressure. The flattening behavior of 5052 aluminum alloy tube has been discussed in our published paper [16], and it presented that the wrinkles cannot be flattened completely when the internal pressures in wrinkling stage are 1.2 p_s, 1.4 p_s, and 1.6 p_s, while they can be flattened completely without any dead wrinkle formation and have a full contact with the die cavity when the internal pressure reaches 1.8 p_s.

For 304 stainless steel tube, there are no dead wrinkles when the internal pressure for wrinkling is 0.6 p_s, 0.8 p_s, 1.0 p_s, and 1.2 p_s, and the flattening shows the best at 1.2 p_s. If a higher internal pressure of 1.4 p_s for wrinkling is used, folding is produced at the die entrance after flattening process. The geometry and size of wrinkles between 5052 aluminum alloy tubes and 304 stainless steel tubes have already been compared when the wrinkling internal pressure was 1.2 p_s and 1.4 p_s in Fig. 15 and Table 3, which showed a big difference between these two tubes regarding the shape of wrinkles. Generally, the flattening process of wrinkles in calibration process is actually a process in which the tube materials move toward different directions under the internal pressure. Now that the geometry and size of wrinkles between 5052 aluminum alloy tubes and 304 stainless

Table 3 Fitting functions for the wrinkles' shape of 5052 aluminum alloy and 304 stainless steel tubes

p_i	Tube	Left wrinkle	Middle wrinkle	Right wrinkle
1.2 p_s	5052	$y = 31.679 + 7.818\exp\left[-\frac{(x+38.356)^2}{53.018}\right]$	$y = 32.454 + 9.540\exp\left[-\frac{(x+0.038)^2}{62.612}\right]$	$y = 31.672 + 8.082\exp\left[-\frac{(x-38.495)^2}{52.547}\right]$
	304	$y = 31.470 + 9.368\exp\left[-\frac{(x+33.971)^2}{159.593}\right]$	$y = 34.389 + 8.146\exp\left[-\frac{(x-0.115)^2}{89.523}\right]$	$y = 31.351 + 9.482\exp\left[-\frac{(x-34.213)^2}{161.792}\right]$
1.4 p_s	5052	$y = 31.689 + 7.930\exp\left[-\frac{(x+37.839)^2}{66.691}\right]$	$y = 32.672 + 9.439\exp\left[-\frac{(x+0.074)^2}{71.080}\right]$	$y = 31.790 + 7.418\exp\left[-\frac{(x-39.376)^2}{74.964}\right]$
	304	$y = 31.478 + 10.530\exp\left[-\frac{(x+32.733)^2}{178.545}\right]$	$y = 35.359 + 7.039\exp\left[-\frac{(x+0.004)^2}{100.334}\right]$	$y = 31.576 + 10.388\exp\left[-\frac{(x-32.468)^2}{179.168}\right]$

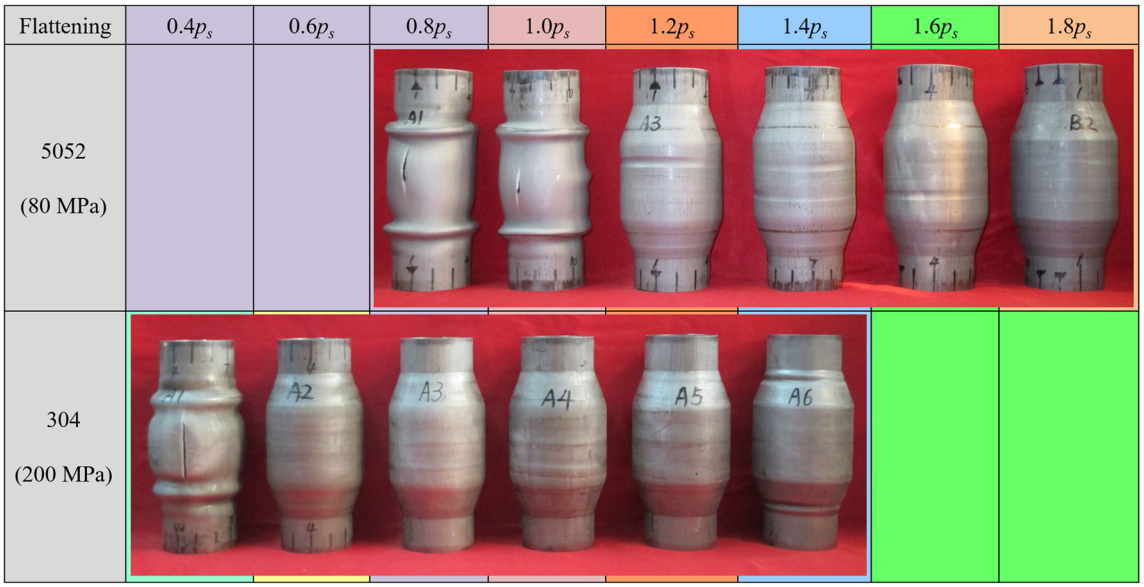

Fig. 16 Effect of mechanical property parameters on the flattening behavior of wrinkles

steel tubes are different, the traveling direction of the tube materials during flattening process will be different, so their flattening behavior will be different.

4 Conclusions

In this paper, the effect of mechanical property parameters on the wrinkling behavior of thin-walled tubes was investigated. Firstly, the effects of elastic modulus, initial yield stress, and tangent modulus of the tubes on their wrinkling behavior were discussed by the finite element analysis. Then, it was verified experimentally with the wrinkling behavior of 5052 aluminum alloy and 304 stainless steel tubes. Conclusions can be drawn from the above discussion as follows:

(1) It has been found that the number and shape of wrinkles have almost no dependence on the elastic modulus under different internal pressures from 0.4 to 1.8 p_s. The effect of elastic modulus on wrinkling behavior of tubes is very small and ignorable.
(2) Initial yield stress and tangent modulus of tubes have an obvious effect on their wrinkling behavior. With the increase of initial yield stress from 85 to 255 MPa, the internal pressure range for the formation of three axisymmetric wrinkles will be moved to lower internal pressure, and the radii of the wrinkles' both top and bottom increase at the internal pressure of 1.2 p_s. Regarding the effect of tangent modulus, it is exactly the opposite to the effect of the increase of initial yield stress. Therefore, tubes with higher initial yield stress and lower tangent modulus tend to possess three wrinkles within the lower internal pressure range.
(3) Three wrinkles can be produced in the internal pressure range of 1.2 to 1.8 p_s for the 5052 aluminum alloy tubes, but this internal pressure range for the 304 stainless steel tubes is moved to the range of 0.6 to 1.4 p_s. When the internal pressure for 5052 and 304 tubes are 1.8 and 1.2 p_s respectively, their wrinkles can be flattened completely.
(4) The ratio of initial yield stress to flow stress of the tubes, σ_s/σ_f, is a significant factor to their wrinkling behavior. The shape and size of the wrinkles are almost the same for the tubes with same value of σ_s/σ_f, and the internal pressure for the formation of three wrinkles will be reduced for the tubes with higher σ_s/σ_f.

Funding information This study was financially supported by National Natural Science Foundation of China (Grant No: 51805357, U1637209). The authors wish to express their gratitude for these funding.

References

1. Benedyk JC (2010) 3 - Aluminum alloys for lightweight automotive structures. In: Mallick PK (ed) Materials, design and manufacturing for lightweight vehicles. Woodhead Publishing, pp 79–113. https://doi.org/10.1533/9781845697822.1.79
2. Zheng L, Wang Z, Liu Z, Song H (2018) Formability and performance of 6K21-T4 aluminum automobile panels in VPF under variable blank holder force. Int J Adv Manuf Technol 94:571–584. https://doi.org/10.1007/s00170-017-0835-7
3. Kulekci MK (2008) Magnesium and its alloys applications in automotive industry. Int J Adv Manuf Technol 39:851–865. https://doi.org/10.1007/s00170-007-1279-2

4. Powell BR, Krajewski PE, Luo AA (2010) 4 - Magnesium alloys for lightweight powertrains and automotive structures. In: Mallick PK (ed) Materials, design and manufacturing for lightweight vehicles. Woodhead Publishing, pp 114–173 https://doi.org/10.1533/9781845697822.1.114
5. Lang LH, Wang ZR, Kang DC, Yuan SJ, Zhang SH, Danckert J, Nielsen KB (2004) Hydroforming highlights: sheet hydroforming and tube hydroforming. J Mater Process Technol 151:165–177. https://doi.org/10.1016/J.JMATPROTEC.2004.04.032
6. Chu E, Xu Y (2004) Hydroforming of aluminum extrusion tubes for automotive applications. Part I: buckling, wrinkling and bursting analyses of aluminum tubes. Int J Mech Sci 46:263–283. https://doi.org/10.1016/j.ijmecsci.2004.02.014
7. Chu E, Xu Y (2004) Hydroforming of aluminum extrusion tubes for automotive applications. Part II: process window diagram. Int J Mech Sci 46:285–297. https://doi.org/10.1016/j.ijmecsci.2004.02.013
8. Yuan S, Wang X, Liu G, Wang ZR (2007) Control and use of wrinkles in tube hydroforming. J Mater Process Technol 182:6–11. https://doi.org/10.1016/j.jmatprotec.2006.06.007
9. Lang L, Yuan S, Wang X, Wang ZR, Fu Z, Danckert J, Nielsen KB (2004) A study on numerical simulation of hydroforming of aluminum alloy tube. J Mater Process Technol 146:377–388. https://doi.org/10.1016/j.jmatprotec.2003.11.031
10. Lang L, Li H, Yuan S, Danckert J, Nielsen KB (2009) Investigation into the pre-forming's effect during multi-stages of tube hydroforming of aluminum alloy tube by using useful wrinkles. J Mater Process Technol 209:2553–2563. https://doi.org/10.1016/j.jmatprotec.2008.06.027
11. Song WJ, Heo SC, Kim J, Kang BS (2006) Investigation on preformed shape design to improve formability in tube hydroforming process using FEM. J Mater Process Technol 177:658–662. https://doi.org/10.1016/j.jmatprotec.2006.04.084
12. Tang Z, Liu G, He Z, Yuan S (2010) Wrinkling behavior of magnesium alloy tube in warm hydroforming. Trans Nonferrous Met Soc China 20:1288–1293. https://doi.org/10.1016/S1003-6326(09)60292-2
13. Yuan S, Yuan W, Wang X (2006) Effect of wrinkling behavior on formability and thickness distribution in tube hydroforming. J Mater Process Technol 177:668–671. https://doi.org/10.1016/j.jmatprotec.2006.04.101
14. Yuan SJ, Cui X-L, Wang X-S (2015) Investigation into wrinkling behavior of thin-walled 5A02 aluminum alloy tubes under internal and external pressure. Int J Mech Sci 92:245–258. https://doi.org/10.1016/j.ijmecsci.2014.12.017
15. Cui XL, Wang XS, Yuan SJ (2015) Wrinkling behavior in tube hydroforming coupled with internal and external pressure. In: MATEC Web of Conferences 21:06002. https://doi.org/10.1051/matecconf/20152106002
16. Wang X-S, Cui X-L, Yuan SJ (2016) Research on flattening behavior of wrinkled 5A02 aluminum alloy tubes under internal pressure. Int J Adv Manuf Technol 87:1159–1167. https://doi.org/10.1007/s00170-016-8529-0
17. Polmear I, StJohn D, Nie J-F et al (2017) The light metals. Light Alloy:1–29. https://doi.org/10.1016/B978-0-08-099431-4.00001-4
18. Chen Z, Gandhi U, Lee J, Wagoner RH (2016) Variation and consistency of Young's modulus in steel. J Mater Process Technol 227:227–243. https://doi.org/10.1016/J.JMATPROTEC.2015.08.024
19. Vollertsen F, Plancak M (2002) On possibilities for the determination of the coefficient of friction in hydroforming of tubes. J Mater Process Technol 125–126:412–420. https://doi.org/10.1016/S0924-0136(02)00292-3